Adsorption of Amphiphiles at an Oil–Water vs. an Oil–Metal Interface

Girma Biresaw*

Cereal Products and Food Science Research Unit, NCAUR, ARS, USDA, Peoria, Illinois 61604

ABSTRACT: Studies were conducted to investigate whether adsorption of amphiphiles from oil onto a degreased metal can be predicted from knowledge about adsorption of the amphiphiles at the oil–water interface. The surface of a degreased metal comprises oxides, hydroxides, and adsorbed water vapor, which form from the reaction of the metal with air and moisture. If the behaviors of amphiphiles at water–oil and metal–oil interfaces are similar, this information can be useful in the development of cheaper and quicker methods of estimating amphiphile adsorption properties on degreased metals. The amphiphiles used were safflower oil (SA) and jojoba oil (JO), both of which are plant-based oils, and methyl palmitate (MP). SA is a triester whereas JO and MP are monoesters. The interfacial tension of water–hexadecane was measured as a function of amphiphile concentration in hexadecane and used to estimate an interfacial-based free energy of adsorption, ΔG_{ads}. The resulting interfacial-based ΔG_{ads} values for SA were identical to those reported from friction-based adsorption isotherms. The corresponding values for the monoesters were within the range reported from friction-based adsorption isotherms.

Paper no. J11004 in *JAOCS 82*, 285–292 (April 2005).

KEY WORDS: Adsorption isotherms, boundary friction, fractional surface coverage, free energy of adsorption, interfacial tension, jojoba, Langmuir adsorption model, methyl palmitate, safflower oil, technical metal.

Agricultural raw materials are increasingly being developed for use in a variety of nonfood applications (1). These developments exploit the abundance, biodegradability, and nontoxic nature of these materials. A major application area of interest for the development of agricultural products is lubrication, which is currently being met almost exclusively by petroleum-based formulations, including metalworking, hydraulics, gear oils, greases, and motor oils (2,3).

Vegetable oils are of particular interest in lubricant development because they are liquid at room temperature and are also amphiphilic, i.e., they contain distinct polar and nonpolar regions within the same molecule. As a result, they can be used as both base oils and film strength/boundary additives in lubricant development. Most vegetable oils are TG (4), of which the polar regions are triesters and the nonpolar regions are the hydrocarbon chains of the FA components. The chemistry of the TG vegetable oils varies depending on the properties of the hydrocarbon chain, such as chain length, degree of unsaturation, stereochemistry, and type and number of other functional groups. Some vegetable oils, such as jojoba, are monoesters of long-chain FA and long-chain fatty alcohols (5).

To develop a lubricant for a specific application, one must first understand the lubrication mechanism for the specific need or application. Most lubrication processes occur in one of the following three categories of lubrication regimes (2): (i) hydrodynamic regime—where the process occurs at high speed and low loads, and the friction surfaces are separated by a thick lubricant film; (ii) boundary regime—where the process occurs at low speed and high load, with the friction surfaces separated by the film-strength additives adsorbed on the rubbing surfaces; and (iii) mixed film regime—where the process occurs at intermediate speed and load, and friction surfaces are separated by a lubricant film in some areas, and by adsorbed film-strength additives in other areas.

In boundary lubrication, the additive adsorbs on the tool and workpiece surface, thereby preventing their direct contact. As a result, the boundary additive allows metalworking to proceed without the tool damaging the workpiece (e.g., galling), and the workpiece causing excessive wear to the tool. To accomplish these goals, the additive must be capable of strongly adsorbing onto the tool and workpiece surfaces and resisting desorption caused by changes in temperature, pressure, or shear. In addition, the additive must be chemically stable, i.e., should not oxidize, decompose, react, or polymerize at the interface during lubrication. Chemical instability not only interferes with adsorption and lubrication but also can cause stains and other defects on the workpiece, thereby negatively affecting product quality.

One way of evaluating the effectiveness of boundary additives is by measuring their free energy of adsorption (ΔG_{ads}) on the friction surfaces of interest (6–9). ΔG_{ads} has been found to be a function of the chemistry of the boundary additive. There are various methods of estimating ΔG_{ads} of boundary additives, all of which involve adsorbing the boundary additive from a solution onto the friction surfaces and measuring the surface concentration of the additive by some technique (gravimetry, spectroscopy, electrical resistance, friction) (6–9). In all cases, the surface concentration increases with increasing concentration of the additive in solution, until full surface coverage is attained. The data are then analyzed using an appropriate adsorption model, from which ΔG_{ads} is obtained.

*Address correspondence at Cereal Products and Food Science Research Unit, NCAUR, ARS, USDA, 1815 N. University St., Peoria, IL 61604. E-mail: biresawg@ncaur.usda.gov

One of the most widely used techniques for measuring ΔG_{ads} was developed by Jahanmir and Beltzer (6), and will be referred to in this manuscript as the friction method. In this method, the boundary coefficient of friction of the additive in the base oil of choice is used to quantify surface concentration. The friction method gives acceptable ΔG_{ads} results for a number of lubricant boundary additives (6–8,10–12), but it is also time consuming and expensive. The method requires, at a minimum, duplicate measurements of boundary friction at several additive concentrations. Therefore, a large number of rather expensive specimens are needed. The objective of this work was to investigate the characteristics of a cheaper alternative to the friction method, termed the interfacial method. The interfacial method is based on a detailed understanding of the chemistry of metallic friction surfaces. If successful, the interfacial method will allow for faster and cheaper estimation of ΔG_{ads} of amphiphiles on metal surfaces. Details of the interfacial method along with some preliminary results are presented herein.

MATERIALS AND METHODS

Materials. Deionized water was purified to a conductivity of 18.3 megohm-cm on a Barnstead EASYpure UV/UF water purification system (model #D8611, EASYpure UV/UF; Barnstead International, Dubuque, IA). Freshly purified water was filtered through a 0.22-μL sterile disposable filter (MILLEX-GS 0.22 μL Filter Unit; Millipore Corporation, Bedford, MA) prior to use in interfacial measurements. Hexadecane (HX) (99+% anhydrous; Aldrich Chemical Co., Milwaukee, WI), safflower oil (SA) (Liberty Vegetable Oil Co., Santa Fe Springs, CA), and methyl palmitate (MP) (99+%; Aldrich Chemical Co.), were used as supplied. Jojoba oil (JO) was obtained from NCAUR and used as supplied. SA is a TG vegetable oil, whereas JO is a monoester vegetable oil comprising a long-chain FA and long-chain fatty alcohols (5). The three esters used in this work, namely, SA, JO, and MP, have M.W. of 864, 606, and 270, respectively, and will be referred to as amphiphiles.

Dynamic interfacial tension measurement. Dynamic interfacial tension was measured using an axisymmetric drop shape analysis (ADSA) method (13). In ADSA, interfacial tension is obtained by analyzing the change in the shape of a pendant drop of one liquid that is suspended in a medium of a second liquid.

Basic concept of the ADSA method. The interfacial tension between a pendant drop of liquid and its surrounding medium, illustrated in Figure 1a, is related to the drop geometry by the Bashforth–Adams equation (9,14):

$$\gamma = (\Delta\rho g a^2)/H \qquad [1]$$

where γ is interfacial tension; $\Delta\rho$ is $(\rho_1 - \rho_2)$, the difference between the densities of the drop and the medium; g is gravitational acceleration; a is the maximum or equatorial diameter of the drop (see Fig. 1a); and H is a drop shape parameter.

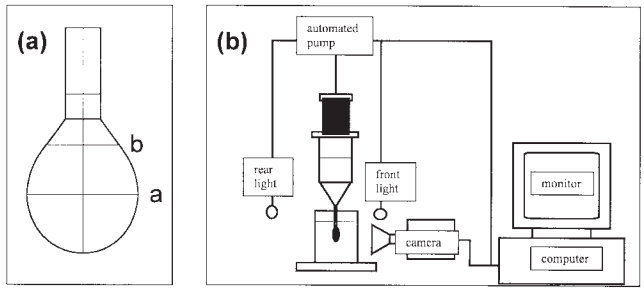

FIG. 1. Schematics of (a) pendant drop, (b) automated goniometer.

The drop shape parameter H is a function of the drop shape factor S, which is calculated from the geometry of the drop as follows:

$$S = b/a \qquad [2]$$

where b is the diameter of the drop at height a from the bottom of the pendant drop (see Fig. 1a).

During dynamic interfacial tension measurement, the geometry of the drop continuously changes as more and more amphiphiles diffuse from the bulk to the interface, thereby changing the interfacial tension. Equilibrium geometry and, hence, equilibrium interfacial tension (IT) are attained when the interface becomes fully saturated with the amphiphiles. In ADSA, the image of the drop is recorded as a function of time with a high-speed camera. At the end of the experiment, image analysis software is used to accurately measure the drop dimensions a and b from each image, and interfacial tension is then calculated automatically by inserting these dimensions into Equations 1 and 2. Further details about the ADSA method appear in Reference 13.

Dynamic interfacial tension measurement instrument and procedure. Dynamic interfacial tension was measured using the FTA 200 automated goniometer (First Ten Angstroms, Portsmouth, VA). The instrument comprises hardware and software that allow for the measurement of contact angle, surface tension, and interfacial tension. A schematic of the instrument hardware configured for dynamic interfacial tension measurement on a pendant drop is shown in Figure 1b. The main features of the hardware relevant to the present work are an automated pump that can be fitted with various sizes of syringes and needles to allow for control of pendant drop formation; a CCD camera (Sanyo B/W CCD Camera model VCB-3512T) that is part of an automated image viewing and capturing system; a computer that acquires, stores, and manipulates data; and a monitor that aids viewing of pendant drop images and data. The instrument software (fta32 v2.0; First Ten Angstroms) is used to carry out various tasks including: setting the experimental conditions (such as maximum drop volume, liquid pump rate, image capture triggering options, total run time, total number of images to be captured, rate of image capture in images/s); acquiring and storing images; calculating interfacial tension by analyzing each image; storing and displaying the results of each image analysis; and storing and displaying the time vs. interfacial tension data for the run.

Dynamic interfacial tension was measured between water and solutions of the amphiphiles (SA, JO, or MP) in HX. The concentrations of the amphiphiles in HX varied from 0.00 (pure HX) to 0.40 M. All measurements were conducted at room temperature (23 ± 2°C) using the FTA-200 automated goniometer equipped with the fta32 v2.0 software. In a typical procedure, a 10-mL disposable syringe (Becton Dickinson & Co., Franklin Lakes, NJ), equipped with a 17-gauge (1.499 mm o.d.) blunt disposable needle (KDS 17-1P; Kahnetics Dispensing Systems, Bloomington, CA) was used to generate a pendant drop of water in an HX medium contained in a glass cuvette (10-mm glass spectrophotometer cell, model 22153D; A. Daigger & Company, Vernon Hills, IL). The syringe was locked into place so that the end of the needle was under the surface of the HX. A manual trigger was used to start the pump so that a few drops of water fell to the bottom of the cuvette. The instrument was then programmed to deliver a specified volume of water automatically at 1 μL/s and to trigger image capture automatically when the pump stopped. The volume of water to be automatically pumped was selected so as to generate the largest possible pendant drop that would not fall before the image acquisition was completed. All runs were programmed to acquire images at a rate of 0.067 s/image, with a post-trigger-period multiplier of 1.27× between images. This allowed for the capture of 35 images during a total acquisition period of 835.6 s. At the end of the acquisition period, each image was automatically analyzed, and a plot of time vs. interfacial tension was automatically displayed. The data from each run were recorded as both a spreadsheet and a video recording. The spreadsheet contained the time and interfacial tension for each image, and the video contained each of the drop images as well as calibration information. Repeat measurements were conducted on each sample, and average values were used in data analysis.

Before running tests with solutions of amphiphiles in HX, the instrument was calibrated with water and then checked by measuring the interfacial tension between water and pure HX.

IT. IT values used in the estimation of ΔG_{ads} were obtained from consecutive dynamic interfacial tension measurements, by averaging the interfacial tension values at very long times, where the interfacial tension attains equilibrium and shows little or no change with time.

RESULTS AND DISCUSSION

The surface of "technical" metals. Technical metals are the workpieces that are commonly used in the manufacture of metallic articles. They can be pure metals or alloys of iron, copper, aluminum, and the like. The metalworking process of the manufacturing step can also vary and can be processes such as machining, grinding, and rolling. A degreased technical metal is one that has been cleaned so that the surface is free of residual lubricants and other organic matter. Degreased technical metals are sometimes referred to as "A wettable" metals (15). Regardless of their metallic composition and manufacturing process, degreased technical metals have certain common features that are important in lubrication. These similarities become apparent when one examines cross sections of various degreased technical metals, all of which display three regions with distinct features (2,16): (i) *Bulk*, or below a depth of 5 μm from the surface. This region has chemical and physical properties that are characteristics of the technical metal. (ii) *Subsurface layer*, at a depth of 1–5 μm from the surface. This region has different chemical and/or physical characteristics from that of the bulk. This difference can be morphological (e.g., grain size and/or shape) and/or chemical (e.g., enrichment by a certain alloying element). For example, the subsurface of heat-treated 5000 series aluminum alloy is richer in Mg than that of the bulk (17). (iii) *Surface layer*, the outermost layer, up to a depth of 10 nm (2). This layer comprises reaction products of the metal with air and moisture, including oxides, hydroxides, and adsorbed water vapor. As such, this layer is hydrophilic and accounts for the excellent water-wettability of degreased technical metals.

A drop of oil placed on a degreased technical metal will form an interface with the surface layer of the metal. Because of the hydrophilicity of the surface layer, it is conceivable that the metal–oil interface will resemble the water–oil interface. This means that one can learn about interactions at the metal–oil interface by investigating interactions at the water–oil interface. This work is aimed at exploring this possibility. To accomplish this, we investigated the adsorption properties of plant-based amphiphiles at the water–oil interface using interfacial measurements. The resulting free energies of adsorption were then compared with those based on adsorption studies of the same amphiphiles at the metal–oil interface.

Effect of amphiphile on HX–water interfacial tension. Figure 2A shows replicate measurements of the dynamic interfacial tension between pure HX and water. The water–HX interfacial tension remained constant for the duration of the measurement period. Table 1 compares the average interfacial tension from the data in Figure 2A with values from the literature (18), as well as those predicted from the surface tension parameters of water and HX (19,20) using current interfacial models (21). As can be seen in Table 1, the average interfacial tension of water–HX obtained from this work using ADSA is similar to the literature value (18). Also, the measured values were similar to values predicted from the surface tension parameters of the two liquids by using the geometric mean and the harmonic mean models (21). However, the Antonoff model (21) underestimated the water–HX interfacial tension.

Solubilization of the amphiphiles in HX results in values of water–HX interfacial tension that are time dependent. This is illustrated in Figure 2B, which shows the interfacial tension vs. time profile between water and HX with a 0.004 M concentration of MP. The interfacial tension profile shows a fast drop in the first few seconds, followed by a gradual decrease over a long period of time, and a more or less constant value toward the end (800 s). The constant interfacial tension at the end corresponds to the IT and is obtained by averaging the last data points of two consecutive runs. Similar time–interfacial tension profiles are obtained with all the amphiphiles and at all concentrations.

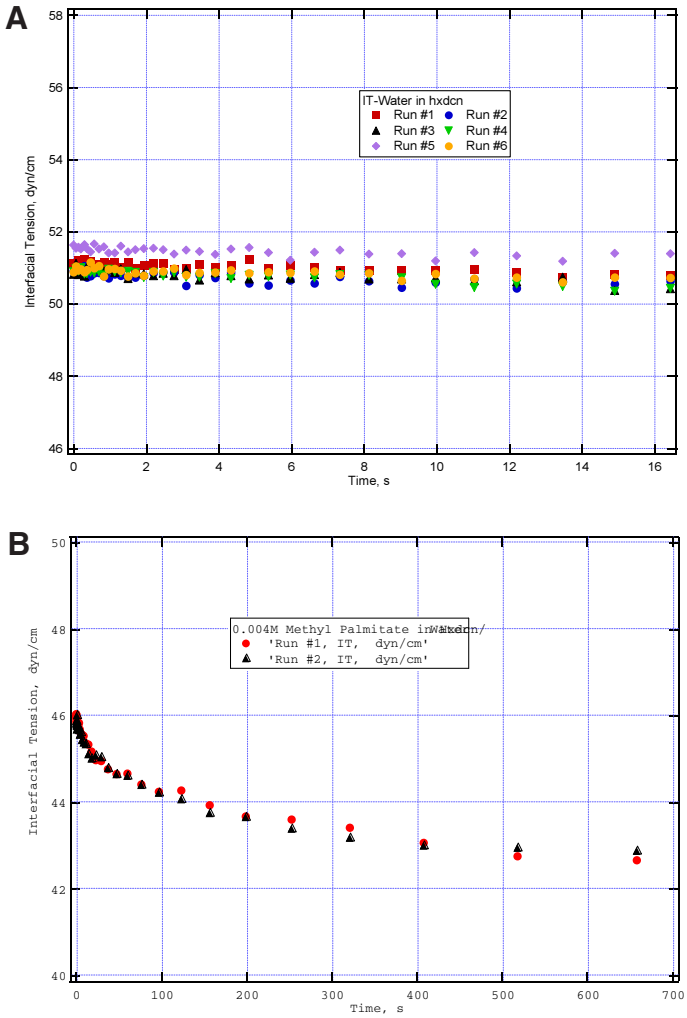

FIG. 2. Dynamic interfacial tension (IT) between water and (A) neat hexadecane (Hxdcn), and (B) Hxdcn with 0.004 M methyl palmitate.

The time dependence of the water–HX interfacial tension in the presence of amphiphiles is caused by the diffusion of the amphiphiles from the bulk HX solution to the water–HX interface. Initially, the interface is almost free of amphiphiles and shows a high interfacial tension value close to that of pure HX–water interface. However, with time, more and more amphiphiles diffuse to the interface, thereby reducing the interfacial tension. After a long time, the interface becomes fully saturated with amphiphiles and the interfacial tension attains an equilibrium value that is independent of time.

TABLE 1
Measured vs. Predicted Interfacial Tensions of Hexadecane (HX)–Water[a]

		HX	Water	HX–Water	Reference
Surface tension (dyn/cm)	Total	27.5	72.8		19,20
	Disp	27.5	21.8		19,20
	Polar	0	51		19,20
Interfacial tension (dyn/cm)	Measured–ADSA			50.7 ± 0.3	This work
	Reported			51.3	18
	Calc–GM			51.3	This work
	Calc–HM			51.7	This work
	Calc–Antonoff			45.3	This work

[a]Disp, dispersion component of surface tension; Polar, polar component of surface tension; Calc, calculated; ADSA, axisymmetric drop shape analysis; GM, geometric mean method; HM, harmonic mean method; Antonoff, Antonoff method (21).

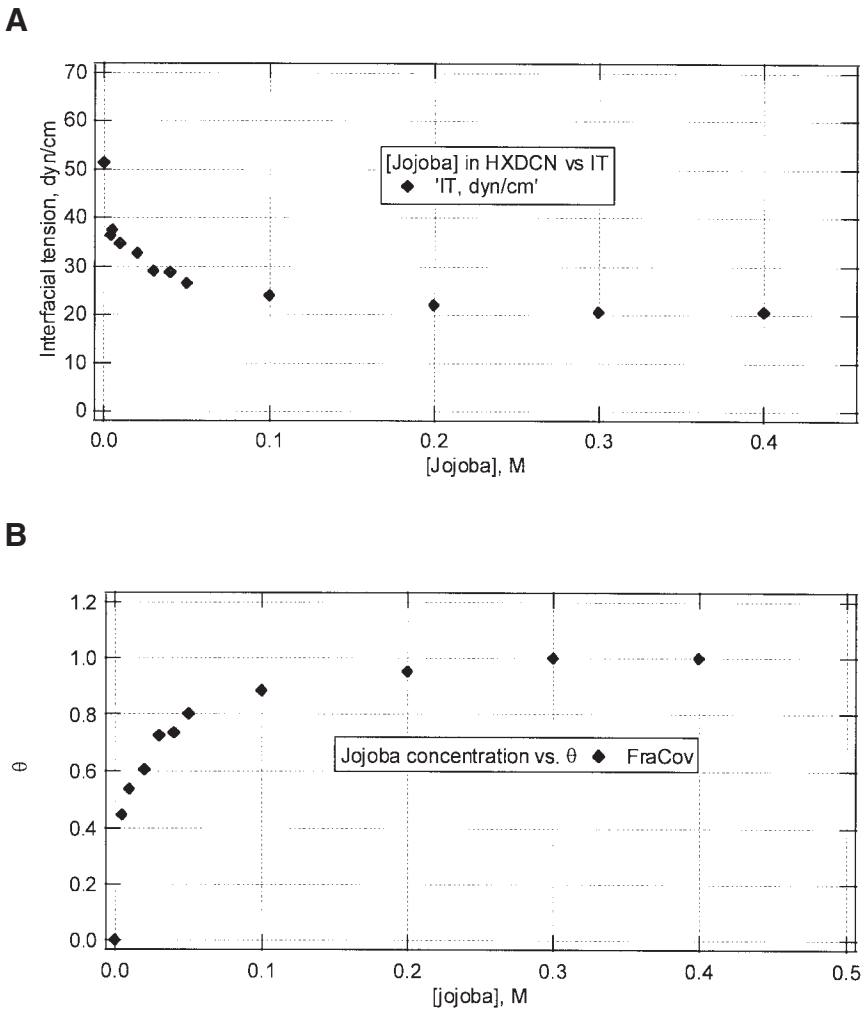

FIG. 3. Effect of jojoba concentration in hexadecane (HXDCN) on (A) water–HXDCN equilibrium interfacial tension (IT), and (B) fractional surface coverage (FraCov).

The value of IT is related to the equilibrium amphiphile concentration at the interface. The latter in turn is a function of the bulk concentration of amphiphile in HX. Thus, increasing the bulk concentration of amphiphile increases the concentration of the amphiphile at the interface and reduces the water–HX interfacial tension. The effect of the bulk amphiphile concentration on interfacial tension is particularly dramatic at low concentrations. This is illustrated in Figure 3A, which shows the effect of jojoba concentration in HX on the IT of water–HX. In the low amphiphile concentration region, addition of amphiphile to HX results in a dramatic reduction in IT (Fig. 3A). Further increase in concentration of amphiphile results in gradual reduction of IT, which levels off at a very high concentration of amphiphile. Similar results are obtained for solutions of SA and MP in HX.

Estimation of free energy of adsorption from HX–water interfacial tension. The free energy of adsorption, ΔG_{ads}, of the amphiphiles at the water–HX interface is obtained by analyzing the adsorption isotherm of the amphiphile using appropriate adsorption models (9). Thus, the first step in this process is that of constructing an adsorption isotherm for each of the amphiphiles investigated. An adsorption isotherm shows the relationship between the concentration of the amphiphile at the interface and that in solution, i.e., in HX. The surface concentration of the amphiphile is expressed in terms of fractional surface coverage, θ, and is obtained from the IT as follows:

$$\theta = (IT_b - IT_i)/(IT_b - IT_a) \quad [3]$$

where IT_b is the IT at the water–HX interface, in the absence of solubilized amphiphile; IT_a is the equilibrium water–HX interfacial tension at full coverage of the interface by the amphiphile; and IT_i is the equilibrium water–HX interfacial tension at amphiphile concentrations below that at full interface coverage.

In Equation 3, IT_b is constant and has a value of 50.7 ± 0.3 (Table 1). IT_a is also constant and unique to each amphiphile. It is the minimum IT of the amphiphile and is obtained from a

TABLE 2
Parameters Used to Calculate Fractional Surface Coverage, θ, from HX–Water Equilibrium Interfacial Tension (IT) Data[a]

System	IT_b (dyn/cm)	IT_a (dyn/cm)
Water–HX	50.7	
Water–HX/safflower oil		21.3
Water–HX/jojoba oil		20.5
Water–HX/methyl palmitate		29.4

[a]IT_b, equilibrium interfacial tension at the water–HX interface in the absence of solubilized amphiphile; IT_a, equilibrium water–HX interfacial tension at full coverage of the interface by the amphilphile. For other abbreviation see Table 1.

plot of the amphiphile concentration vs. IT data such as that shown in Figure 3A. IT_a values for SA, JO, and MP obtained from the corresponding data are summarized in Table 2.

The concentration vs. IT data for each amphiphile (similar to those shown in Fig. 3A) and (IT_a, IT_b) data shown in Table 2 were used in Equation 3 to calculate θ. The resulting data were then used to construct an adsorption isotherm, which is a plot of amphiphile concentration in HX vs. θ. Figure 3B shows such a plot for jojoba. In this figure, the plot of amphiphile concentration vs. θ is a mirror image of the concentration vs. IT plot in Figure 3A. The adsorption isotherms for the other amphiphiles showed similar profiles.

To determine the free energy of adsorption, ΔG_{ads}, the adsorption isotherms were analyzed using the Langmuir adsorption model (9). The Langmuir model predicts the following relationship between the concentration of the amphiphile in solution, C, and that at the interface, θ:

$$\theta = (K_o C)/(1 + K_o C) \quad [4]$$

TABLE 3
Parameters Used to Calculate Fractional Surface Coverage, θ, from HX–Water IT Data[a]

Amphiphile	K_0 (M^{-1})	ΔG_{ads} (kcal/mol)
Safflower	528	–3.70
Jojoba	162	–3.00
Methyl palmitate	179	–3.06

[a]For abbreviations see Tables 1 and 2.

or

$$1/\theta = 1 + 1/(K_o C) \quad [5]$$

where K_o is the equilibrium constant, expressed in mol^{-1}. According to the Langmuir model, plots of ($1/C$) vs. ($1/\theta$) will give a straight line with an intercept of 1 and a slope of ($1/K_o$). The resulting K_o is then used to calculate the free energy of adsorption, ΔG_{ads}, in kcal/mol, as follows:

$$\Delta G_{ads} = -RT \ln(K_o) \quad [6]$$

where R is the universal gas constant, 1.987×10^{-3} kcal/mol K, and T is temperature, in degrees K.

The adsorption isotherms for JO, MP, and SA were analyzed according to Equation 5. An example of such analysis is given in Figure 4, which shows the Langmuir analysis of the adsorption isotherm for SA. The ($1/C$) vs. ($1/\theta$) plot for SA showed a linear relationship, with an intercept around 1. Similar results were observed for the other amphiphiles. From the slopes of the lines, the values of K_o were calculated and used to obtain ΔG_{ads} of the amphiphiles using Equation 6. The results of the Langmuir analysis for the three amphiphiles are summarized in Table 3.

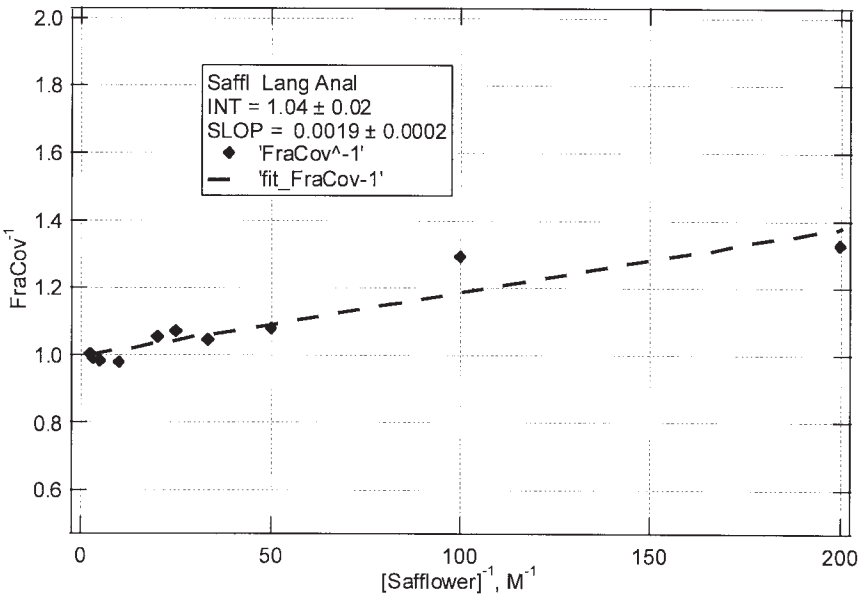

FIG. 4. Langmuir analysis of the adsorption isotherm of safflower oil at the water–hexadecane interface (INT). SLOP, slope; for other abbreviation see Figure 3.

TABLE 4
Comparison of ΔG_{ads} from Langmuir Analysis of Friction-Based vs. Interfacial-Based Adsorption Isotherms (kcal/mol)

Amphiphiles	Experimental method	ΔG_{ads}	Reference
Safflower	Interfacial/HX–Water	−3.70	This work
Safflower	Friction/ball-on-disk[a]	−3.65	10
Jojoba	Interfacial/HX–Water	−3.00	This work
Jojoba	Friction/ball-on-disk[a]	−3.27	10
Methyl palmitate	Interfacial/HX–Water	−3.06	This work
Methyl palmitate	Friction/ball-on-disk[a]	−2.70	10

[a]Steel/steel. For abbreviation see Table 1.

Interfacial- vs. friction-based free energy of adsorption. Examination of Table 3 indicates that the interfacial-based free energy of adsorption at the water–HX interface increases in the order SA < MP = JO. The fact that SA adsorbs more strongly to the interface than the other two amphiphiles is consistent with the difference in the chemistries between SA and the other amphiphiles. SA is a triester (TG), whereas MP and JO are monoesters. As a result, SA can engage in multiple bonding at the interface, whereas the monoesters can only engage in single bonding. It is proposed that the observed stronger adsorption of SA is due to multiple H-bonding between SA and the water at the interface. The monoesters MP and JO can only engage in a single H-bonding with water. Consequently, MP and JO will have relatively weaker adsorption at the interface. Similar results have been observed in previous studies comparing the relative adsorption properties of monoesters vs. triesters on metal surfaces (10).

Comparison of the ΔG_{ads} of JO vs. that for MP in Table 3, however, shows little difference in their adsorption properties, despite the big difference in their M.W. (see the Materials and Methods section, first paragraph). JO is a monoester of long-chain (C_{16}–C_{24}) FA and long-chain (C_{18}–C_{24}) fatty alcohols (5), whereas MP is a monoester of C_{16} FA and methanol. It appears that the difference in the chemistries of the monoesters does not significantly affect their adsorption properties at the water–HX interface.

Table 4 compares the ΔG_{ads} values of the amphiphiles from this work, which are obtained from Langmuir analysis of interfacial-based adsorption isotherms, with those obtained from similar analysis of friction-based adsorption isotherms (10). Both methods predict stronger adsorption of SA to the interface than the monoesters. This has been attributed to the ability of SA to engage in multiple bonding at the interface, which is not possible with the monoesters. The data in Table 4 also show that the two methods give similar values of ΔG_{ads} for SA. Thus, the interfacial-based method apparently is a quick and cheap alternative to the friction-based method for estimating the adsorption properties of TG amphiphiles from oil onto metal surfaces.

As shown in Table 4, relative to the friction-based method, the interfacial-based method seems to slightly overestimate the adsorption properties of MP and slightly underestimate those of JO. In both cases, the difference between the two methods is about 0.3 kcal/mol. Because of this difference, the friction method predicts stronger adsorption of JO than MP, whereas the interfacial method predicts a more or less similar degree of adsorption by the two monoester amphiphiles.

ACKNOWLEDGMENTS

The author gratefully acknowledges Megan Goers for help with the interfacial tension measurements, Dr. Thomas Abbott for providing sample of jojoba, and Dr. Edwin B. Bagley for reviewing and commenting on this manuscript.

REFERENCES

1. Lawton, J.W., Nonfood Uses of Cereals, in *Handbook of Cereal Science and Technology*, 2nd edn., edited by K. Kulp and J.G. Ponte, Marcel Dekker, New York, 2000, pp. 725–740.
2. Schey, J.A., *Tribology in Metalworking Friction, Lubrication and Wear,* American Society of Metals, Metals Park, OH, 1983, pp. 27–130.
3. Dwivedi, M.C., and S. Sapre, Total Vegetable-Oil Based Greases Prepared from Castor Oil, *J. Synth. Lubr. 19*:229–241 (2002).
4. Bockish, M., *Fats and Oils Handbook*, AOCS Press, Champaign, IL, 1998.
5. Miwa, T.K., Structural Determination and Uses of Jojoba Oil, *J. Am. Oil Chem. Soc. 61*:407–410 (1984).
6. Jahanmir, S., and M. Beltzer, An Adsorption Model for Friction in Boundary Lubrication, *ASLE Trans. 29*:423–430 (1986).
7. Beltzer, M., Assessing Adsorption of Conventional Friction Modifying Molecules by Relative Contact Potential Difference Measurements, *J. Tribol. 114*:675–682 (1992).
8. Biresaw, G., A. Adhvaryu, S.Z. Erhan, and C.J. Carriere, Friction and Adsorption Properties of Normal and High Oleic Soybean Oils, *J. Am. Oil Chem. Soc. 79*:53–58 (2002).
9. Hiemenz, P.C., *Principles of Colloid and Surface Chemistry*, 2nd edn., Marcel Dekker, New York, 1986.
10. Biresaw, G., A. Adhvaryu, and S.Z. Erhan, Friction Properties of Vegetable Oils, *J. Am. Oil Chem. Soc. 80*:697–704 (2003).
11. Jahanmir, S., and M. Beltzer, Effect of Additive Molecular Structure on Friction Coefficient and Adsorption, *J. Tribol. 108*:109–116 (1986).
12. Beltzer, M., and S. Jahanmir, Role of Dispersion Interactions Between Hydrocarbon Chains in Boundary Lubrication, *ASLE Trans. 30*:47–54 (1987).

13. Rotenberg, Y., L. Boruvka, and A.W. Neumann, Determination of Surface Tension and Contact Angle from the Shapes of Axisymmetric Fluid Interfaces, *J. Colloid Interface Sci. 93*:169–183 (1983).
14. Adamson, A.P., and A.W. Gast, *Physical Chemistry of Surfaces*, John Wiley & Sons, New York, 1997.
15. Strohmeier, B.R., Testing and Improving the Wettability of Aluminum Foil, Part 1, *Aluminium 68*:892–896 (1992).
16. Wefers, K., and C. Misra, *Oxides and Hydroxides,* Alcoa Technical Paper No. 19, Revised, Alcoa Laboratories, Alcoa Center, PA, 1987.
17. Wakefield, G.R., and R.M. Sharp, The Composition of Oxides Formed on Al-Mg Alloys, *Appl. Surf. Sci. 51*:95–102 (1991).
18. van Oss, C.J., M.K. Chaudhury, and R.J. Good, Monopolar Surfaces, *Adv. Colloid Interface Sci. 28*:35–64 (1987).
19. Jasper, J.J., The Surface Tension of Pure Liquid Compounds, *J. Phys. Chem. Ref. Data 1*:841–1009 (1972).
20. van Oss, C.J., *Interfacial Forces in Aqueous Media*, Marcel Dekker, New York, 1994.
21. Wu, S., *Polymer Interface and Adhesion*, Marcel Dekker, New York, 1982.

[Received December 7, 2004; accepted March 14, 2005]